Anal. Chem. **2010,** *82,* 2048–2058

High-Resolution Desorption Electrospray Ionization Mass Spectrometry for Chemical Characterization of Organic Aerosols

Julia Laskin,*,† Alexander Laskin,*,‡ Patrick J. Roach,† Gordon W. Slysz,§ Gordon A. Anderson,§ Sergey A. Nizkorodov,⊥ David L. Bones,⊥ and Lucas Q. Nguyen⊥

Chemical and Materials Sciences Division, Pacific Northwest National Laboratory, P.O. Box 999, MSIN K8-88, Richland, Washington 99352, William R. Wiley Environmental Molecular Sciences Laboratory, Pacific Northwest National Laboratory, P.O. Box 999, MSIN K8-88, Richland, Washington 99352, Biological Sciences Division, Pacific Northwest National Laboratory, P.O. Box 999, MSIN K8-88, Richland, Washington 99352, and Department of Chemistry, University of California−Irvine, Irvine, California 92697

Characterization of the chemical composition and chemical transformations of secondary organic aerosol (SOA) is both a major challenge and the area of greatest uncertainty in current aerosol research. This study presents the first application of desorption electrospray ionization combined with high-resolution mass spectrometry (DESI-MS) for detailed chemical characterization and studies of chemical aging of organic aerosol (OA) samples collected on Teflon substrates. DESI-MS offers unique advantages both for detailed characterization of chemically labile components in OA that cannot be detected using traditional electrospray ionization mass spectrometry (ESI-MS) and for studying chemical aging of OA. DESI-MS enables rapid characterization of OA samples collected on substrates by eliminating the sample preparation stage. In addition, it enables detection and structural characterization of chemically labile molecules in OA samples by minimizing the residence time of analyte in the solvent. In this study, DESI-MS and tandem mass spectrometry experiments (MS/MS) were used to examine chemical aging of SOA produced by the ozonolysis of limonene (LSOA) in the presence of gaseous ammonia. Exposure of LSOA to ammonia resulted in measurable changes in the optical properties of the sample observed using ultraviolet (UV)−visible spectroscopy. High-resolution DESI-MS analysis demonstrated that chemical aging results in formation of highly conjugated nitrogen-containing species that are most likely responsible for light-absorbing properties of the aged LSOA. Detailed analysis of the experimental data allowed us to identify several key aging reactions, including the transformation of carbonyls to imines, intramolecular dimerization of imines with other carbonyl compounds in SOA, and intermolecular cyclization of imines. This study presents an important step toward understanding the formation of light-absorbing OA (brown carbon) in the atmosphere.

Atmospheric particles have a significant impact on climate via their interactions with incoming solar radiation and modifications of cloud properties.[1−6] The extent of radiative forcing and cloud condensation caused by aerosols is an area of significant uncertainty in global and regional climate modeling. This uncertainty is a consequence of the significant variation of physical and chemical properties of tropospheric aerosols on local and regional scales[7] and the substantial time evolution of these properties as a result of atmospheric aerosol chemistry (aging).[8] An accurate assessment of the environmental impact of aerosols requires a fundamental understanding of the relationship between their composition and chemical and physical properties. However, because atmospheric particles typically consist of a complex mixture of compounds with a wide range of molecular weights, structures, physical properties, and chemical reactivity, detailed characterization of their chemical composition is challenging.

Both in situ and offline methods of aerosol analyses are utilized for characterization of the physical and chemical properties of atmospheric particles. In situ techniques including single-particle mass spectrometry (SPMS) and aerosol mass spectrometry (AMS) enable real-time analysis of the size-dependent composition of aerosols.[9−12] A variety of offline microscopy, microprobe, and

* Authors to whom correspondence should be addressed. E-mail addresses: Julia.Laskin@pnl.gov (J.L.), Alexander.Laskin@pnl.gov (A.L.). Tel.: 509-371-6136; Fax: 509-371-6072; URL: http://emslbios.pnl.gov/id/laskin_j (J.L.). Tel.: 509-371-6129; Fax: 509-371-6039; URL: http://emslbios.pnl.gov/id/laskin_a (A.L.).

† Chemical and Materials Sciences Division, Pacific Northwest National Laboratory.

‡ William R. Wiley Environmental Molecular Sciences Laboratory, Pacific Northwest National Laboratory.

§ Biological Sciences Division, Pacific Northwest National Laboratory.

⊥ Department of Chemistry, University of California−Irvine.

(1) Seinfeld, J. H.; Pankow, J. F. *Annu. Rev. Phys. Chem.* **2003**, *54*, 121–140.
(2) Poschl, U. *Angew. Chem., Int. Ed.* **2005**, *44*, 7520–7540.
(3) Simoneit, B. R. T. *Appl. Geochem.* **2002**, *17*, 129–162.
(4) Andreae, M. O.; Rosenfeld, D. *Earth-Sci. Rev.* **2008**, *89*, 13–41.
(5) Rosenfeld, D.; Lohmann, U.; Raga, G. B.; O'Dowd, C. D.; Kulmala, M.; Fuzzi, S.; Reissell, A.; Andreae, M. O. *Science* **2008**, *321*, 1309–1313.
(6) Unger, N.; Shindell, D. T.; Koch, D. M.; Streets, D. G. *J. Geophys. Res.* **2008**, *113*, D02306 (DOI: 10.1029/2007JD008683).
(7) Zhang, Q.; Jimenez, J. L.; Canagaratna, M. R.; Allan, J. D.; Coe, H.; Ulbrich, I.; Alfarra, M. R.; Takami, A.; Middlebrook, A. M.; Sun, Y. L.; Dzepina, K.; Dunlea, E.; Docherty, K.; DeCarlo, P. F.; Salcedo, D.; Onasch, T.; Jayne, J. T.; Miyoshi, T.; Shimono, A.; Hatakeyama, S.; Takegawa, N.; Kondo, Y.; Schneider, J.; Drewnick, F.; Borrmann, S.; Weimer, S.; Demerjian, K.; Williams, P.; Bower, K.; Bahreini, R.; Cottrell, L.; Griffin, R. J.; Rautiainen, J.; Sun, J. Y.; Zhang, Y. M.; Worsnop, D. R. *Geophys. Res. Lett.* **2007**, *34*, L13801 (DOI: 10.1029/2007GL029979).
(8) Rudich, Y.; Donahue, N. M.; Mentel, T. F. *Annu. Rev. Phys. Chem.* **2007**, *58*, 321–352.
(9) Wexler, A. S.; Johnston, M. V. Real-Time Single-Particle Analysis. In *Aerosol Measurement—Principles, Techniques, and Applications*; Willeke, K., Baron, P. A., Eds.; John Wiley & Sons, Ltd.: New York, 2001.
(10) Noble, C. A.; Prather, K. A. *Mass Spectrom. Rev.* **2000**, *19*, 248–274.
(11) Canagaratna, M. R.; Jayne, J. T.; Jimenez, J. L.; Allan, J. D.; Alfarra, M. R.; Zhang, Q.; Onasch, T. B.; Drewnick, F.; Coe, H.; Middlebrook, A.; Delia, A.; Williams, L. R.; Trimborn, A. M.; Northway, M. J.; DeCarlo, P. F.; Kolb, C. E.; Davidovits, P.; Worsnop, D. R. *Mass Spectrom. Rev.* **2007**, *26*, 185–222.

10.1021/ac902801f
Published on Web 02/10/2010

microspectroscopy techniques have also been used extensively for the chemical characterization of individual particles.[13−16] Single-particle methods provide important information on sizes, densities, number concentrations, chemical types, and morphologies of individual particles. However, their ability to characterize chemical composition at a molecular level of detail is limited, because of the complexity of aerosol samples and the highly destructive nature of vaporization and ionization used in single-particle sampling. Detailed molecular composition is usually inferred from the complementary analysis of bulk aerosol samples.[1,17]

Characterization of the molecular composition and chemical transformations of organic aerosol (OA) is particularly challenging; typically only 10−20% of the total OA mass can be successfully identified and quantified using traditional gas chromatography−mass spectrometry (GC-MS) analysis.[8,18−21] It has been suggested that the unidentified fraction of OA consists of high-molecular-weight compounds that cannot be detected using GC-MS.[8] Electrospray ionization mass spectrometry (ESI-MS) is a valuable tool for the analysis of polar molecules of any size.[22−26] However, the high complexity of aerosol samples results in a significant number of isobaric interferences in ESI-MS spectra that complicate the assignment of individual features based on the low-resolution mass analysis. One approach to dealing with this problem involves coupling of ESI-MS with liquid chromatographic (LC) separation,[27−29] although the loss of a significant fraction of the OA constituents in the separation column is a major drawback of LC methods. An alternative highly promising approach relies on high-resolution mass spectrometry (HR-MS).[30−42] The high mass resolving power of HR-MS enables simultaneous identification of hundreds or even thousands of organic species without the need for LC separation providing a unique insight on the chemical composition of OA.

In ESI-MS studies, OA samples collected on substrates are extracted into solvents for subsequent analysis. It has been recently demonstrated[37] that solvent−analyte reactions can significantly alter the composition of aerosol extracts and possibly complicate identification of aerosol constituents. Specifically, reactions of methanol with carbonyl and carboxyl groups of organic compounds present in OA may result in formation of hemiacetals, acetals, and esters on time scales ranging from several minutes to several days. Possible alterations of OA constituents during the extraction stage can be alleviated by ionizing the sample directly from the substrate.

The recent development of atmospheric pressure surface ionization techniques enables rapid and sensitive characterization of samples in their native environment without sample preparation.[43−45] A variety of atmospheric pressure surface ionization techniques has been developed since the initial report by Cooks and co-workers in 2004.[46] These include desorption electrospray ionization (DESI),[43,46,47] in which ions are formed during collisions of electrically charged droplets with the substrate; direct analysis in real time (DART),[48] which utilizes a plasma of excited-state atoms and ions for simultaneous desorption and ionization of molecules from the surface of a sample; desorption atmospheric pressure chemical ionization (DAPCI);[49] electrospray-assisted

(12) Zelenyuk, A.; Imre, D. *Int. Rev. Phys. Chem.* **2009**, *28*, 309–358.
(13) De Bock, L. A.; Van Grieken, R. E. Single particle analysis techniques. In *Analytical Chemistry of Aerosols*; Spurny, K. R., Ed.; Lewis Publishers, Ltd.: Boca Raton, FL, 1999.
(14) Buseck, P. R.; Posfai, M. *Proc. Natl. Acad. Sci. U.S.A.* **1999**, *96*, 3372–3379.
(15) Fletcher, R. A.; Small, J. A.; Scott, J. H. J. Analysis of individual collected particles. In *Aerosol Measurement—Principles, Techniques, and Applications*, Willeke, K., Baron, P. A., Eds.; John Wiley & Sons, Ltd.: New York, 2001.
(16) Laskin, A.; Cowin, J. P.; Iedema, M. J. *J. Electron Spectrosc. Relat. Phenom.* **2006**, *150*, 260–274.
(17) Solomon, P. A.; Norris, G.; Landis, M.; Tolocka, M. Chemical Analysis Methods for Atmospheric Aerosol Components. In *Aerosol Measurement—Principles, Techniques, and Applications*; Willeke, K., Baron, P. A., Eds.; John Wiley & Sons, Ltd.: New York, 2001.
(18) Rogge, W. F.; Hildemann, L. M.; Mazurek, M. A.; Cass, G. R.; Simoneit, B. R. T. *Environ. Sci. Technol.* **1998**, *32*, 13–22.
(19) Falkovich, A. H.; Graber, E. R.; Schkolnik, G.; Rudich, Y.; Maenhaut, W.; Artaxo, P. *Atmos. Chem. Phys.* **2005**, *5*, 781–797.
(20) Hoffer, A.; Gelencser, A.; Blazso, M.; Guyon, P.; Artaxo, P.; Andreae, M. O. *Atmos. Chem. Phys.* **2006**, *6*, 3505–3515.
(21) Rudich, Y. *Chem. Rev.* **2003**, *103*, 5097–5124.
(22) Fenn, J. B.; Mann, M.; Meng, C. K.; Wong, S. F.; Whitehouse, C. M. *Science* **1989**, *246*, 64–67.
(23) Marshall, A. G.; Rodgers, R. P. *Acc. Chem. Res.* **2004**, *37*, 53–59.
(24) Bogdanov, B.; Smith, R. D. *Mass Spectrom. Rev.* **2005**, *24*, 168–200.
(25) Feng, X.; Siegel, M. M. *Anal. Bioanal. Chem.* **2007**, *389*, 1341–1363.
(26) Panda, S. K.; Andersson, J. T.; Schrader, W. *Anal. Bioanal. Chem.* **2007**, *389*, 1329–1339.
(27) Warnke, J.; Bandur, R.; Hoffmann, T. *Anal. Bioanal. Chem* **2006**, *385*, 34–45.
(28) Reinnig, M. C.; Muller, L.; Warnke, J.; Hoffmann, T. *Anal. Bioanal. Chem.* **2008**, *391*, 171–182.
(29) Winterhalter, R.; Herrmann, F.; Kanawati, B.; Nguyen, T. L.; Peeters, J.; Vereecken, L.; Moortgat, G. K. *Phys. Chem. Chem. Phys.* **2009**, *11*, 4152–4172.
(30) Tolocka, M. P.; Jang, M.; Ginter, J. M.; Cox, F. J.; Kamens, R. M.; Johnston, M. V. *Environ. Sci. Technol.* **2004**, *38*, 1428–1434.
(31) Kalberer, M.; Paulsen, D.; Sax, M.; Steinbacher, M.; Dommen, J.; Prevot, A. S. H.; Fisseha, R.; Weingartner, E.; Frankevich, V.; Zenobi, R.; Baltensperger, U. *Science* **2004**, *303*, 1659–1662.
(32) Reemtsma, T.; These, A.; Venkatachari, P.; Xia, X. Y.; Hopke, P. K.; Springer, A.; Linscheid, M. *Anal. Chem.* **2006**, *78*, 8299–8304.
(33) Surratt, J. D.; Murphy, S. M.; Kroll, J. H.; Ng, N. L.; Hildebrandt, L.; Sorooshian, A.; Szmigielski, R.; Vermeylen, R.; Maenhaut, W.; Claeys, M.; Flagan, R. C.; Seinfeld, J. H. *J. Phys. Chem. A* **2006**, *110*, 9665–9690.
(34) Reinhardt, A.; Emmenegger, C.; Gerrits, B.; Panse, C.; Dommen, J.; Baltensperger, U.; Zenobi, R.; Kalberer, M. *Anal. Chem.* **2007**, *79*, 4074–4082.
(35) Walser, M. L.; Desyaterik, Y.; Laskin, J.; Laskin, A.; Nizkorodov, S. A. *Phys. Chem. Chem. Phys.* **2008**, *10*, 1009–1022.
(36) Altieri, K. E.; Seitzinger, S. P.; Carlton, A. G.; Turpin, B. J.; Klein, G. C.; Marshall, A. G. *Atmos. Environ.* **2008**, *42*, 1476–1490.
(37) Bateman, A. P.; Walser, M. L.; Desyaterik, Y.; Laskin, J.; Laskin, A.; Nizkorodov, S. A. *Environ. Sci. Technol.* **2008**, *42*, 7341–7346.
(38) Wozniak, A. S.; Bauer, J. E.; Sleighter, R. L.; Dickhut, R. M.; Hatcher, P. G. *Atmos. Chem. Phys.* **2008**, *8*, 5099–5111.
(39) Smith, J. S.; Laskin, A.; Laskin, J. *Anal. Chem.* **2009**, *81*, 1512–1521.
(40) Laskin, A.; Smith, J. S.; Laskin, J. *Environ. Sci. Technol.* **2009**, *43*, 3764–3771.
(41) Heaton, K. J.; Sleighter, R. L.; Hatcher, P. G.; Hall, W. A., IV.; Johnston, M. V. *Environ. Sci. Technol.* **2009**, *43*, 7797–7802.
(42) Bateman, A. P.; Nizkorodov, S. A.; Laskin, J.; Laskin, A. *Phys. Chem. Chem. Phys.* **2009**, *11*, 7931–7942.
(43) Cooks, R. G.; Ouyang, Z.; Takats, Z.; Wiseman, J. M. *Science* **2006**, *311*, 1566–1570.
(44) Van Berkel, G. J.; Pasilis, S. P.; Ovchinnikova, O. *J. Mass Spectrom.* **2008**, *43*, 1161–1180.
(45) Chen, H.; Gamez, G.; Zenobi, R. *J. Am. Soc. Mass. Spectrom.* **2009**, *20*, 1947–1963.
(46) Takats, Z.; Wiseman, J. M.; Gologan, B.; Cooks, R. G. *Science* **2004**, *306*, 471–473.
(47) Takats, Z.; Wiseman, J. M.; Cooks, R. G. *J. Mass Spectrom.* **2005**, *40*, 1261–1275.
(48) Cody, R. B.; Laramee, J. A.; Durst, H. D. *Anal. Chem.* **2005**, *77*, 2297–2302.

laser desorption ionization (ELDI);[50] and several hyphenated techniques.[51−53]

DESI-MS has been widely used for rapid detection and analysis of chemical warfare agents and explosives,[49,54,55] pharmaceutical samples,[56] counterfeit drugs[57] and drugs of abuse,[58] biological fluids and tissues,[59,60] and chemical imaging of a variety of surfaces.[61−63] Despite the widespread use of this ionization technique, it has been only recently applied for the analysis of OA samples collected on substrates.[64,65] Yang and co-workers demonstrated the utility of DESI-MS for rapid quantitative detection of carboxylic acids[65] and polycyclic aromatic hydrocarbons[64] in samples of particulate matter.

In this study, we report first high-resolution mass spectrometry (HR-MS) characterization of the chemical composition of laboratory-generated OA using DESI-MS combined with MS/MS fragmentation experiments of selected ions. We show that high-resolution DESI-MS provides unique information on the composition of aerosol samples that cannot be obtained using ESI-MS. We demonstrate this by examining chemical transformations associated with gas-to-particle reactions of OA and ammonia, which are relevant to the formation of light-absorbing (brown) carbon in the atmospheric environment. In addition to rapid analysis that does not require any sample preparation besides the collection of aerosol on a substrate, DESI provides an important advantage of short residence time of OA constituents in solvent droplets, which minimizes solution-phase dissociation of labile organic compounds present in OA. Rapid and gentle analysis of OA samples using DESI-MS allowed us to identify highly conjugated N-containing organic compounds, which are most likely responsible for the absorption of the visible light by the aged OA.

EXPERIMENTAL SECTION

Preparation and Collection of Organic Aerosol Samples. Secondary organic aerosol particles produced from the ozonolysis of D-limonene vapors (LSOA), as described in our previous studies,[35,42] were collected onto Teflon substrates using a 10- stage micro-orifice uniform deposit impactor (MOUDI) (Model 110R, MSP, Inc.). The principles of operation of MOUDI can be found elsewhere.[66] Freshly prepared LSOA samples of size-selected particles of 0.18−0.32 μm aerodynamic diameter collected on the eighth impactor stage were characterized using DESI-MS and ESI-MS. For aging experiments, the sample was placed onto a plastic plate and exposed to the gas-phase mixture of NH_3, HNO_3, and H_2O by floating the plate in a covered Petri dish containing 0.1 M aqueous solution of NH_4NO_3 (Aldrich, Inc., 99.99% purity). Equilibrium partial pressures of NH_3, HNO_3, and H_2O were calculated using an extended Aerosol Inorganic Model (AIM) Model II[67] available on the web (http://www.aim.env.uea.ac.uk/aim). The calculated equilibrium partial pressures of NH_3(g) and HNO(g) are 1.2×10^{-7} atm and 1.6×10^{-13} atm, respectively. For a typical relative humidity (RH) of ca. 85% inside the Petri dish, real concentrations of NH_3(g) and HNO_3(g) are somewhat lower. Because the partial pressure of NH_3 is much higher than of HNO_3, the observed aerosol aging is mainly attributed to reactions between organic constituents of LSOA with ammonia. The concentration of NH_3 used in this study (ca. 100 ppb) is significantly higher than typical concentrations of ammonia in the atmosphere (0.1−10 ppb)[68] but is lower than high ambient concentrations of 200 ppb[69] observed in some urban areas and 0.5−1.5 ppm[70] in forest fire plumes.

Ultraviolet (UV)−Visible Spectroscopy. Gas-to-particle reactions in the aging experiments were accompanied by a gradual change of the sample color from white to brown as the aging proceeded. This change was characterized via a series of UV−visible measurements. LSOA was collected on calcium fluoride (CaF_2) windows placed on modified substrate holders in MOUDI. After collection, the CaF_2 window with deposited SOA was attached to one end of a glass absorption cell, and the other end was sealed with a clean window. The cell was connected to a bubbler containing a solution of 0.1 M NH_4NO_3 in water and placed inside a dual-beam UV−visible spectrometer (Shimadzu, Model 2450). UV−visible spectra were collected using two separated clean CaF_2 windows as reference. The LSOA on the window was continuously exposed to equilibrium concentrations of NH_3(g) and HNO_3(g) at ca. 85% RH. Transmission spectra were recorded hourly for 20 h in the 220−700 nm range.

Mass Spectrometry. Samples were analyzed using a high-resolution LTQ-Orbitrap mass spectrometer (Thermo Electron, Bremen, Germany) with a modified electrospray ionization (ESI) or desorption electrospray ionization (DESI) source (Prosolia, Inc.,

(49) Takats, Z.; Cotte-Rodriguez, I.; Talaty, N.; Chen, H. W.; Cooks, R. G. *Chem. Commun.* **2005**, 1950–1952, DOI: 10.1039/b418697d.
(50) Shiea, J.; Huang, M. Z.; Hsu, H. J.; Lee, C. Y.; Yuan, C. H.; Beech, I.; Sunner, J. *Rapid Commun. Mass Spectrom.* **2005**, *19*, 3701–3704.
(51) Sampson, J. S.; Hawkridge, A. M.; Muddiman, D. C. *J. Am. Soc. Mass. Spectrom.* **2006**, *17*, 1712–1716.
(52) Nyadong, L.; Galhena, A. S.; Fernandez, F. M. *Anal. Chem.* **2009**, *81*, 7788–7794.
(53) Cheng, S. C.; Cheng, T. L.; Chang, H. C.; Shiea, J. *Anal. Chem.* **2009**, *81*, 868–874.
(54) Cotte-Rodriguez, I.; Takats, Z.; Talaty, N.; Chen, H. W.; Cooks, R. G. *Anal. Chem.* **2005**, *77*, 6755–6764.
(55) Ifa, D. R.; Jackson, A. U.; Paglia, G.; Cooks, R. G. *Anal. Bioanal. Chem.* **2009**, *394*, 1995–2008.
(56) Chen, H. W.; Talaty, N. N.; Takats, Z.; Cooks, R. G. *Anal. Chem.* **2005**, *77*, 6915–6927.
(57) Newton, P. N.; Green, M. D.; Fernandez, F. M.; Day, N. P. J.; White, N. J. *Lancet Infect. Dis.* **2006**, *6*, 602–613.
(58) Rodriguez-Cruz, S. E. *Rapid Commun. Mass Spectrom.* **2006**, *20*, 53–60.
(59) Wiseman, J. M.; Ifa, D. R.; Song, Q. Y.; Cooks, R. G. *Angew. Chem., Int. Ed.* **2006**, *45*, 7188–7192.
(60) Kauppila, T. J.; Talaty, N.; Kuuranne, T.; Kotiaho, T.; Kostiainen, R.; Cooks, R. G. *Analyst* **2007**, *132*, 868–875.
(61) Van Berkel, G. J.; Kertesz, V. *Anal. Chem.* **2006**, *78*, 4938–4944.
(62) Lane, A. L.; Nyadong, L.; Galhena, A. S.; Shearer, T. L.; Stout, E. P.; Parry, R. M.; Kwasnik, M.; Wang, M. D.; Hay, M. E.; Fernandez, F. M.; Kubanek, J. *Proc. Natl. Acad. Sci. U.S.A.* **2009**, *106*, 7314–7319.
(63) Sampson, J. S.; Hawkridge, A. M.; Muddiman, D. C. *J. Am. Soc. Mass. Spectrom.* **2008**, *19*, 1527–1534.
(64) Li, M.; Chen, H.; Wang, B. F.; Yang, X.; Lian, J. J.; Chen, J. M. *Int. J. Mass Spectrom.* **2009**, *281*, 31–36.
(65) Li, M.; Chen, H.; Yang, X.; Chen, J. M.; Li, C. L. *Atmos. Environ.* **2009**, *43*, 2717–2720.
(66) Marple, V. A.; Rubow, K. L.; Behm, S. M. *Aerosol Sci. Technol.* **1991**, *14*, 434–446.
(67) Clegg, S. L.; Brimblecombe, P.; Wexler, A. S. *J. Phys. Chem. A* **1998**, *102*, 2137–2154.
(68) Seinfeld, J. H.; Pandis, S. N. *Atmospheric Chemistry and Physics*; John Wiley & Sons: New York, 1998.
(69) Li, Y. Q.; Schwab, J. J.; Demerjian, K. L. *J. Geophys. Res.* **2006**, *111*, D10S02 (DOI: 10.1029/2005JD006275).
(70) Griffith, D. W. T.; Mankin, W. G.; Coffey, M. T.; Ward, D. E.; Riebau, A. In *Global Biomass Burning*; Levine, J. S., Ed.; MIT Press: Cambridge, MA, 1991; pp. 230−239.

Indianapolis, IN). For ESI experiments, solvent extracts were prepared by ultrasonic washing of the Teflon substrates in 1 mL of acetonitrile. The extracts were filtered using Whatman 0.45 μm Teflon (polytetrafluoroethylene, PTFE) membrane disposable filters. Samples were injected through a pulled fused-silica capillary (50 μm inner diameter) at a flow rate of 0.3−1.0 μL/min, using a spray voltage of 3.5−4.2 kV. Between each sample run, the capillary was flushed multiple times with methanol to remove residual compounds. DESI experiments were performed for samples collected on Teflon substrates using the following conditions: spray voltage of 4 keV, 1 mm distance from the spray needle to the surface, 50° angle between the spray needle and the surface normal, 1 mm distance between the heated capillary of the LTQ/Orbitrap and the substrate, 2−3 mm distance between the spray needle and the capillary. The system was operated in the positive-ion mode with a resolving power of 60 000 at m/z 400. The instrument was calibrated using a standard mixture of caffeine, MRFA, and Ultramark 1621 (calibration mix MSCAL 5, Sigma−Aldrich, Inc.). Background spectra were obtained by analyzing blank Teflon substrates using the same experimental procedures.

Mass spectral features with the signal-to-noise ratio of 3 and higher were extracted from raw spectra using Decon2LS[71] and subsequently clustered using the VIPER program[72] that were developed at Pacific Northwest National Laboratory (PNNL) (http://ncrr.pnl.gov/software/). Clustering of mass spectra aligns signal intensities observed in experimental spectra along a common m/z axis to facilitate peak identification and comparison of spectral data obtained for different samples or settings. Clustering was performed using mass tolerance of 5 ppm for m/z < 250 and 3 ppm for higher masses. Clustered spectral features were organized into a table using an Excel macro. Background peaks were subsequently eliminated. The remaining peaks were assigned probable empirical formulas using freeware programs Formula Calculator v. 1.1 (http://magnet.fsu.edu/~midas/download.html) and Molecular Weight Calculator (http://ncrr.pnl.gov/software/), as well as through the use of Kendrick diagrams.[73−75] Molecular formulas searches included the following elements: C (up to 100 atoms), H (up to 100 atoms), N (up to 8 atoms), O (up to 25 atoms), and Na (up to 1 atom).

Kendrick transformation aids in the identification and categorization of homologous compounds by normalizing the experimental mass-to-charge value to the nominal mass of a chemical group (e.g., CH_2, O, CH_2O, etc.). Oxygen-based Kendrick diagrams were most informative for the analysis of samples used in this study. For the O-Kendrick diagram, the Kendrick mass (KM_O) is calculated by renormalizing the International Union of Pure and Applied Chemistry (IUPAC) mass scale to the exact mass of oxygen using eq 1:

$$KM_O = \text{observed mass} \times \left(\frac{\text{nominal mass of O}}{\text{exact mass of O}}\right) \quad (1)$$

The Kendrick mass defect (KMD) is calculated as the difference between the nominal mass of an ion and KM_O using eq 2:

$$KMD = \text{nominal mass} - KM_O \quad (2)$$

The nominal mass appearing in eqs 1 and 2 is obtained by rounding the corresponding exact mass to the nearest integer. The advantage of Kendrick analysis is that homologous compounds differing only by the number of base units (e.g., O-atoms in this particular case) have identical KMD values. When the KMD_O values are plotted versus the mass-to-charge ratio of a compound, homologous series or series of compounds differing only by the number of O atoms fall onto horizontal lines and are clearly distinguishable.[73,74] Identification of the elemental composition of one compound in the homologous series enables assignment of all peaks in the series. In this study, all peaks in different O-Kendrick series (except for the leading low-mass member of the series) were identified using Kendrick analysis.

RESULTS AND DISCUSSION

In previous studies, we employed methanol and acetonitrile for the extraction and HR-MS analysis of limonene secondary organic aerosol (LSOA) samples collected on substrates. However, no signal could be obtained by DESI of LSOA samples using these solvents without addition of a strong acid, which was consistent with previous reports on the DESI-MS analysis of aerosol samples.[64,65] Optimal signal was obtained using 1:1 (v:v) mixture of acetonitrile (AcN) and water with 0.1% by volume of trifluoroacetic acid (TFA) denoted AcN/TFA in the text. All spectra reported in this work were acquired in the positive-ion mode. Figure 1a shows the DESI spectrum of the freshly prepared LSOA. An ESI spectrum obtained using the same solvent is shown for comparison on the negative intensity scale. Both spectra contain abundant peaks corresponding to monomeric products of limonene ozonolysis separated by masses of CH_2 and O and a broader pattern corresponding to the formation of dimers, trimers, and tetramers, resembling our previously published data.[35,37,42] Because of the large number of spectral features present in both spectra, it is easier to compare them by plotting the unique features observed in each spectrum. Figure 1b shows the distribution of mass spectral features present only in the DESI spectrum (positive intensities) and only in the ESI spectrum (negative intensities) of the fresh LSOA sample. In both cases, the majority of unique peaks are of low intensity with normalized abundance of 10% or lower, indicating that DESI analysis adequately represents the distribution of organic constituents in the fresh LSOA sample. The most noticeable difference is the larger relative intensity of the oligomeric species in the DESI spectrum (m/z > 300). Peaks that are unique to DESI appear most frequently in the oligomeric mass range.

A recent study by Bones et al.[76] examined chemical aging of SOA produced via the ozonolysis of terpenes. It has been demonstrated that the reactions of SOA constituents extracted into water with ammonia or primary amines resulted in the formation of products that have strong absorption features at

(71) Jaitly, N.; Mayampurath, A.; Littlefield, K.; Adkins, J. N.; Anderson, G. A.; Smith, R. D. *BMC Bioinformatics* **2009**, *10*, 87.
(72) Monroe, M. E.; Tolic, N.; Jaitly, N.; Shaw, J. L.; Adkins, J. N.; Smith, R. D. *Bioinformatics* **2007**, *23*, 2021–2023.
(73) Kendrick, E. *Anal. Chem.* **1963**, *35*, 2146–2154.
(74) Hughey, C. A.; Hendrickson, C. L.; Rodgers, R. P.; Marshall, A. G.; Qian, K. *Anal. Chem.* **2001**, *73*, 4676–4681.
(75) Meija, J. *Anal. Bioanal. Chem.* **2006**, *385*, 486–499.
(76) Bones, D. L.; Henricksen, D. K.; Mang, S. A.; Gonsior, M.; Bateman, A. P.; Nguyen, T. B.; Cooper, W. J.; Nizkorodov, S. A. *J. Geophys. Res.*, **2009**, in press. (DOI: 10.1029/2009JD012864.)

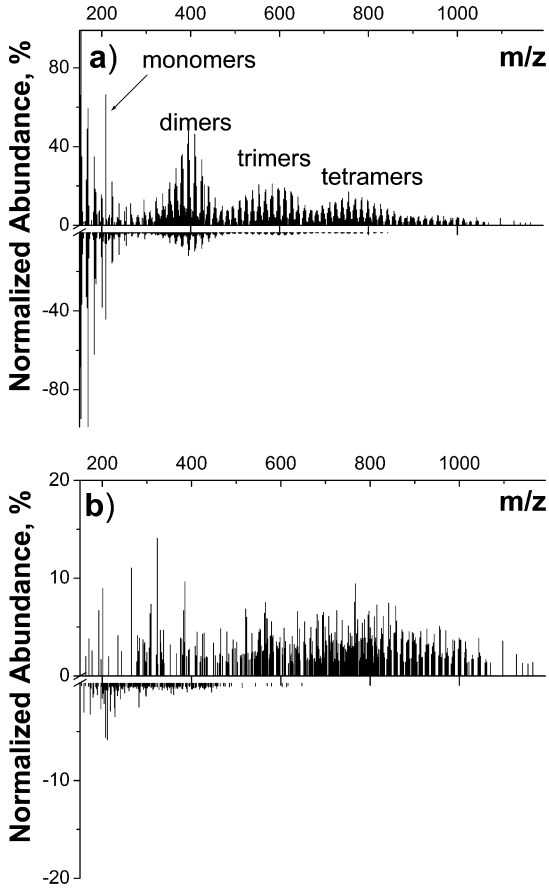

Figure 1. Comparison of the positive-ion mode DESI and ESI spectra of the fresh (white) LSOA sample obtained using AcN/TFA as a solvent. The results are plotted as positive and negative signal for DESI and ESI, respectively: (a) full DESI (positive region of plot) and ESI (negative region of plot) spectra; (b) unique features observed only in DESI (positive) and only in ESI (negative) spectra.

ultraviolet and visible (UV−vis) wavelengths. The presence of nitrogen-containing chromophores in the products of chemical aging was confirmed using UV−vis and fluorescence spectroscopy. However, ESI-MS could not detect any significant difference between the fresh and aged samples suggesting that the chromophores were present at low concentrations in aged SOA samples. The formation of OA capable of absorbing visible light has recently attracted significant attention.[77] It has been commonly assumed that, because OA does not absorb visible light, it has mostly a cooling effect on the climate through scattering of the incoming solar radiation. However, light-absorbing OA—"brown carbon"—has been recently identified as a significant constituent of particulate matter originating from combustion sources and vehicle emissions.[78] The formation of light-absorbing constituents of OA has been also attributed to atmospheric aging processes.[79]

In this study, we examined the chemical composition of reaction products formed in the ammonium-mediated aging of OA, which is one of the processes that can be responsible for the formation of brown carbon.[76] Specifically, we studied LSOA aging by exposing the sample collected on a Teflon substrate to mixed vapors of NH_3, HNO_3, and H_2O (corresponding to their equilibrium partial pressures) over 0.1 M aqueous solution of ammonium nitrate (NH_4NO_3), which is one of the most ubiquitous atmospheric particulate constituents. This approach allowed us to examine chemical transformations resulting from gas-to-particle reactivity of SOA over a 24-h time period.

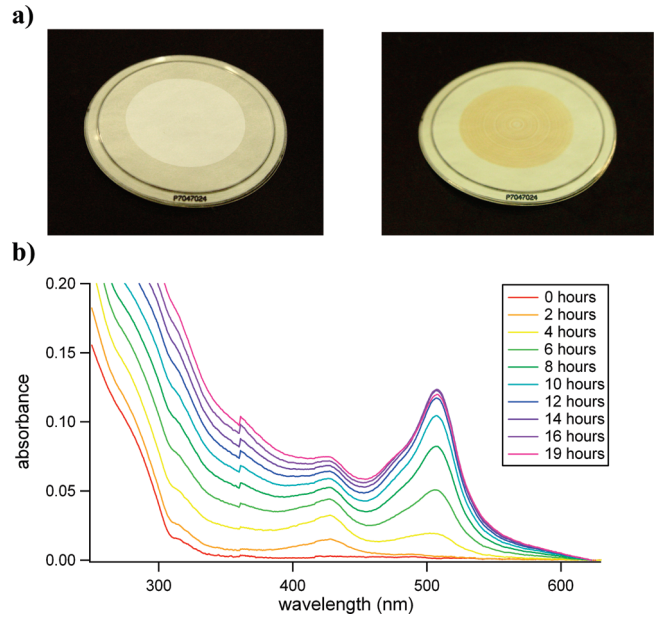

Figure 2. (a) Photographs of the fresh (left) and aged (right) LSOA samples; (b) UV−visible spectra of LSOA, aged on CaF_2 window in the presence of NH_3(g).

Figure 2a shows photographs of the fresh and aged LSOA samples. Clearly, chemical aging results in a substantial change in the color of the LSOA material. Although the fresh LSOA sample is white and is almost indistinguishable from the Teflon substrate, the aged sample has light brown color. UV−visible spectra of SOA on CaF_2 windows show a distinct increase in absorption over time at specific wavelengths (see Figure 2b). Scattering from the particles, which is largely independent of wavelength and decreases with time as the particles absorb ambient water vapor, was also clearly evident. For clarity, the change in the baseline due to scattering was removed from the traces shown in Figure 2b by setting the absorbance at 700 nm to 0. Typically, 2 mg of SOA was deposited uniformly on a 2.5 cm window, resulting in an effective thickness of SOA material of 3×10^{-4} cm on the window. The similarity between the observed change of color in aqueous-phase[76] and heterogeneous gas-to-particle aging of LSOA suggests that both processes involve similar chemical transformations of aerosol constituents.

Figure 3a shows high-resolution DESI and ESI mass spectra of the aged (brown) LSOA sample. At first glance, the spectra look quite similar and show the presence of monomer, dimer, trimer, and tetramer regions, although the relative abundance of higher-mass species is lower than that observed in spectra of the fresh (white) LSOA sample. However, spectra obtained by plotting unique features present only in DESI and only in ESI of the aged sample (Figure 3b) are remarkably different. Specifically, only a few peaks are present exclusively in the ESI spectrum, whereas the DESI spectrum contains more than 800 additional features corresponding to the LSOA aging products. Comparison between DESI spectra of the fresh

(77) Andreae, M. O.; Gelencser, A. *Atmos. Chem. Phys.* **2006**, *6*, 3131–3148.
(78) Jacobson, M. Z. *J. Geophys. Res.* **1999**, *104*, 3527–3542.
(79) Shapiro, E. l.; Szprengiel, J.; Sareen, N.; Jen, C. N.; Giordano, M. R.; McNeill, V. F. *Atmos. Chem. Phys.* **2009**, *9*, 2289–2300.

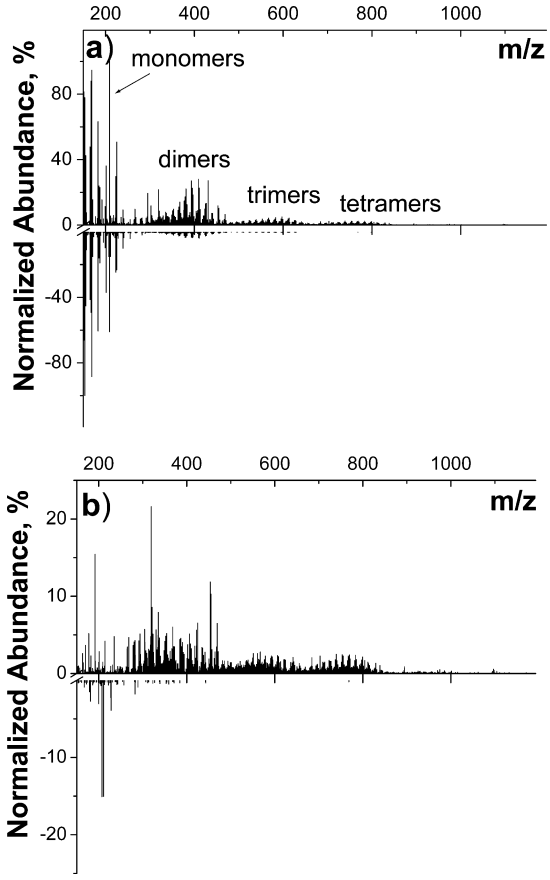

Figure 3. Comparison of the positive-ion mode DESI and ESI spectra of the aged (brown) LSOA sample obtained using AcN/TFA as a solvent (the results are plotted in the positive and negative regions of the plot for DESI and ESI, respectively): (a) full DESI (positive) and ESI (negative) spectra; (b) unique features observed only in DESI (positive) and only in ESI (negative) spectra.

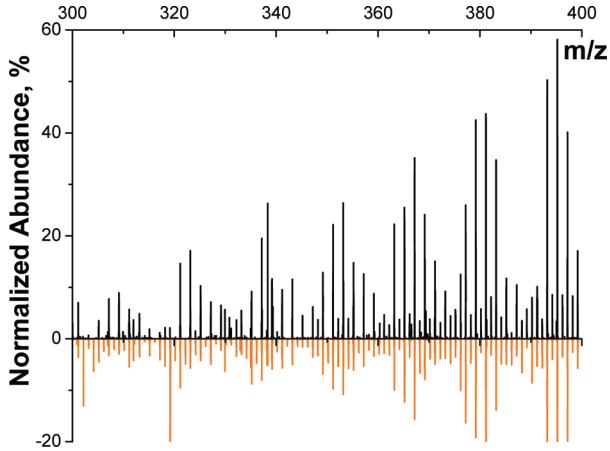

Figure 4. Comparison of a portion of positive-ion mode DESI spectra of the fresh (white) and aged (brown) LSOA samples. The results are plotted as positive (black bars) and negative (orange bars) signals, respectively. The abundance of peaks with even nominal masses corresponding to compounds that contain one N atom increases considerably in the spectrum of the aged sample.

and aged samples shown in Figure 4 demonstrates that a significant number of the new peaks correspond to nitrogen-containing species. Indeed, the majority of peaks in the fresh LSOA sample is composed of C, H, and O atoms and are cationized by sodium. As a result, these peaks have odd nominal masses. Small features observed in the fresh LSOA at even nominal masses correspond to ^{13}C isotopes of the major odd-m/z peaks. In contrast, a significant number of abundant features in the DESI spectrum of the aged LSOA sample have even nominal masses.

Kendrick analysis of the high-resolution data allowed us to assign over 55% of peaks in DESI and ESI spectra. Note that, during peak assignment, we mainly focused on abundant peaks below m/z 600 and peaks clustered into oxygen-based Kendrick series. Table 1 lists the 50 most-abundant reaction products observed in the aged (brown) sample using DESI analysis. Clearly, all newly formed peaks contain one or two N atoms. Interestingly, most nitrogen-containing features are observed as protonated species, whereas the majority of oxygenated organic compounds in the fresh (white) LSOA sample are cationized by sodium. Preferential protonation of nitrogen-containing organic compounds is consistent with the higher proton affinity (PA) of amines and imines, compared to carbonyl compounds that are dominant species in the fresh LSOA sample. Several sodiated species containing one or two N atoms are also observed at m/z above 500.

Bones et al.[76] discussed possible mechanisms of formation of nitrogen-containing organic molecules in aqueous extracts of LSOA mediated by dissolved ammonia ions (NH_4^+). At 85% RH, which was utilized in our aging experiments, the hygroscopic growth factor of LSOA is ~1.1,[80] which suggests that substantial water uptake by LSOA particles occurs under the experimental conditions used in this study. In addition, it has been reported that LSOA particles do not exhibit deliquescence or efflorescence phase transitions, which is indicative of continuous water uptake over a wide range of RH values.[80] It follows that chemical transformations of the LSOA observed in our experiments can be attributed to the hygroscopic uptake of H_2O, NH_3, and HNO_3, followed by chemistry between ammonia and carbonyl functional groups of LSOA constituents occurring in an aqueous film on the surface of the particles.

The acid-catalyzed reaction of aldehydes or ketones with ammonia results in formation of imines (reaction r1). This reaction is accompanied by the loss of one water molecule and is reversible in the presence of acid.

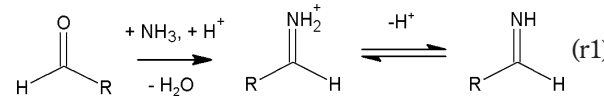

This reaction decreases the molecular weight of the reacting molecule by 0.984 amu: this is the difference between the exact mass of O and NH. A significant number of LSOA constituents contain multiple carbonyl groups[35] that can be converted to imines via reaction r1. Once formed, the imine group can undergo reactions with carbonyls present in the skeleton of the same molecule, forming nitrogen-containing heterocyclic compounds, as illustrated by reaction r2:

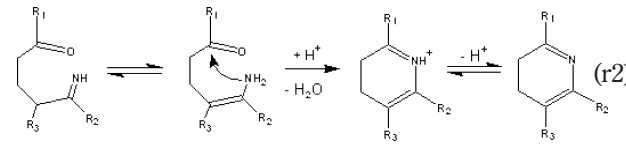

Table 1. The Most-Abundant Nitrogen-Containing Positive Ions Observed in the DESI Spectrum of the Aged (Brown) LSOA Sample

		Signal-to-Noise Ratio					
			ESI of Aged Sample				
m/z	calculated mass of the ion	DESI of aged sample	in AcN	in AcN/TFA	intensity ratio DESI/ESI(AcN)	elemental formula of the ion	DBE
152.1067	152.1075	282	46	0	6.1	$C_9H_{14}NO$	4
166.0860	166.0868	324	201	189	1.6	$C_9H_{12}NO_2$	5
168.1017	168.1024	661	399	231	1.7	$C_9H_{14}NO_2$	4
170.0811	170.0817	74	0	0		$C_8H_{12}NO_3$	4
184.0968	184.0973	190	208	93	0.9	$C_9H_{14}NO_3$	4
186.1124	186.1130	53	30	0	1.8	$C_9H_{16}NO_3$	3
204.1229	204.1235	53	90	0	0.6	$C_9H_{18}NO_4$	2
218.1384	218.1392	121	318	92	0.4	$C_{10}H_{20}NO_4$	2
264.1593	264.1599	64	17	0	3.7	$C_{15}H_{22}NO_3$	6
266.1752	266.1755	196	15	0	12.9	$C_{15}H_{24}NO_3$	5
268.1543	268.1548	95	26	0	3.7	$C_{14}H_{22}NO_4$	5
278.1751	278.1755	74	22	0	3.3	$C_{16}H_{24}NO_3$	6
280.1907	280.1912	83	36	0	2.3	$C_{16}H_{26}NO_3$	5
282.1700	282.1704	87	32	0	2.7	$C_{15}H_{24}NO_4$	5
291.1704	291.1708	86	18	0	4.8	$C_{16}H_{23}N_2O_3$	7
302.1751	302.1755	239	21	0	11.6	$C_{18}H_{24}NO_3$	8
304.1545	304.1548	116	17	0	6.9	$C_{17}H_{22}NO_4$	8
305.1861	305.1864	82	20	0	4.1	$C_{17}H_{25}N_2O_3$	7
313.1912	313.1915	64	0	0		$C_{19}H_{25}N_2O_2$	9
315.1705	315.1708	60	0	0		$C_{18}H_{23}N_2O_3$	9
317.1860	317.1864	74	32	0	2.3	$C_{18}H_{25}N_2O_3$	8
318.1701	318.1704	97	49	0	2.0	$C_{18}H_{24}NO_4$	8
319.2017	319.2020	439	44	0	9.9	$C_{18}H_{27}N_2O_3$	7
320.1858	320.1861	77	89	0	0.9	$C_{18}H_{26}NO_4$	7
321.1810	321.1813	174	22	0	7.8	$C_{17}H_{25}N_2O_4$	7
322.1651	322.1654	56	51	0	1.1	$C_{17}H_{24}NO_5$	7
322.2013	322.2017	90	84	0	1.1	$C_{18}H_{28}NO_4$	6
324.1807	324.1810	55	72	0	0.8	$C_{17}H_{26}NO_5$	6
332.1859	332.1861	62	37	0	1.7	$C_{19}H_{26}NO_4$	8
333.1809	333.1813	52	28	0	1.9	$C_{18}H_{25}N_2O_4$	8
333.2173	333.2177	55	19	0	2.9	$C_{19}H_{29}N_2O_3$	7
334.1653	334.1654	69	47	0	1.4	$C_{18}H_{24}NO_5$	8
335.1964	335.1970	161	45	0	3.6	$C_{18}H_{27}N_2O_4$	7
336.1805	336.1810	86	86	0	1.0	$C_{18}H_{26}NO_5$	7
338.1961	338.1966	94	142	0	0.7	$C_{18}H_{28}NO_5$	6
348.1809	348.1810	60	47	0	1.3	$C_{19}H_{26}NO_5$	8
350.1961	350.1966	85	117	0	0.7	$C_{19}H_{28}NO_5$	7
351.1915	351.1919	52	20	0	2.6	$C_{18}H_{27}N_2O_5$	7
352.1755	352.1759	98	98	0	1.0	$C_{18}H_{26}NO_6$	7
352.2117	352.2123	95	455	0	0.2	$C_{19}H_{30}NO_5$	6
354.1910	354.1916	105	185	0	0.6	$C_{18}H_{28}NO_6$	6
360.2015	360.2021	54	53	0	1.0	$C_{17}H_{30}NO_7$	4
366.1912	366.1916	65	107	0	0.6	$C_{19}H_{28}NO_6$	7
368.2066	368.2072	122	248	0	0.5	$C_{19}H_{30}NO_6$	6
370.1860	370.1865	71	69	0	1.0	$C_{18}H_{28}NO_7$	6
370.2222	370.2228	65	93	0	0.7	$C_{19}H_{32}NO_6$	5
372.2010	372.2021	70	64	0	1.1	$C_{18}H_{30}NO_7$	5
384.2009	384.2021	89	98	0	0.9	$C_{19}H_{30}NO_7$	6
436.2532	436.2545	50	49	0	1.0	$C_{20}H_{38}NO_9$	3
441.2380	441.2388	56	16	0	3.4	$C_{25}H_{33}N_2O_5$	11
453.2747	453.2752	241	33	0	7.3	$C_{27}H_{37}N_2O_4$	11
455.2540	455.2544	208	37	0	5.6	$C_{26}H_{35}N_2O_5$	11
457.2331	457.2337	63	0	0		$C_{25}H_{33}N_2O_6$	11
467.2898	467.2908	70	19	0	3.6	$C_{28}H_{39}N_2O_4$	11
469.2694	469.2701	132	29	0	4.6	$C_{27}H_{37}N_2O_5$	11
471.2484	471.2494	58	17	0	3.4	$C_{26}H_{35}N_2O_6$	11

Reaction r2 results in an additional decrease of the molecular weight of the reacting molecules by 18.0106 amu, which is the exact mass of a water molecule. The combined net effect of reactions r1 and r2 is the decrease of the molecular weight of the LSOA constituents by 18.9946 amu.

Aging products formed via reactions r1 and r2 can combine and undergo disproportionation, as illustrated by reaction r3. This reaction results in formation of two additional products separated from the precursor by the mass of two H atoms (±2.0156 amu).

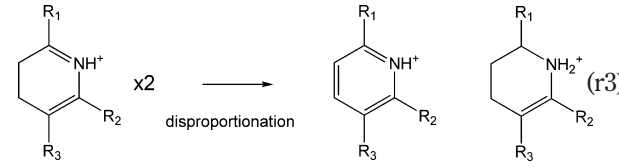

(r3)

Table 2. Distribution of Mass Shifts Corresponding to the Formation of Products of Reactions r1−r3 Observed in DESI Spectra

charge carrier	net gain/loss of atoms	net change in m/z	net change in DBE	Number of Occurrences	
				fresh sample	aged sample
		Reaction r1			
H^+	+NH; −O	−0.9840	0	10	186
Na^+	$+NH_2$; −O; −Na	−22.9660		42	209
		Reaction r2			
H^+	+N; −H; $-O_2$	−18.9946	0	7	154
Na^+	+N; $-O_2$; −Na	−40.9765		14	122
		Reaction r3			
	+2H; −2H	(±) 2.0156	−1; +1	4	264

It has been suggested that substituted dihydropyridinium and pyridinium ions, formed through reactions r2 and r3, respectively, are most likely responsible for the absorption of light with a wavelength of ~500 nm, resulting in the brown color of the aged LSOA samples.[76]

A detailed analysis of high-resolution DESI-MS spectra shows that reactions r1−r3 indeed play a significant role in chemical aging of LSOA constituents. Table 2 shows a summary of the number of occurrences of mass shifts corresponding to reactions r1−r3 observed in DESI spectra of the fresh and aged LSOA samples. The number of products that are consistent with the reactions r1−r3 increases by an order of magnitude at least, as a result of chemical aging. This suggests that a significant number of nitrogen-containing species in the DESI spectrum of the aged LSOA sample can be attributed to reactions r1−r3.

Because reactions r1−r3 are acid-catalyzed and reversible, it is reasonable to assume that the resulting products are unstable during extraction and ESI analysis, especially in the acidified solvent. Indeed, only a small number of nitrogen-containing species were observed in the ESI spectrum obtained using AcN/TFA as a solvent (see Table 1.) This is consistent with the results of Bones et al.,[76] showing that the addition of sulfuric acid inhibits the formation of UV/vis chromophores in aqueous extracts of LSOA. In contrast, the ESI spectrum obtained in this study using pure acetonitrile (ESI/AcN) was much more similar to the DESI spectrum and contained a large number of nitrogen-containing species. However, a close examination of the peak intensities observed in both spectra (see Table 1) reveals that a significant number of nitrogen-containing aging products are suppressed or absent in the ESI/AcN spectrum. Because solvent extracts of LSOA samples are typically slightly acidic, it is reasonable to assume that, even in nonacidified acetonitrile extracts, the equilibrium is shifted toward the reactants. It follows that the relative abundance of nitrogen-containing species produced via reactions r1−r3 may be significantly reduced in an acidic environment (e.g., fogwater[81]). Future studies will examine the dependence of SOA composition on the pH.

The distribution of the number of N and O atoms in DESI spectra of fresh and aged LSOA samples is shown in Figure 5. The fresh (white) sample is mainly composed of organic molecules containing C, H, and O atoms, and contains a small number of species with one N atom (<6%). Nitrogen-containing species in the spectrum of the fresh LSOA sample could originate from reactions with trace amounts of NH_3 in the laboratory air or from reactions of dissolved analyte molecules with acetonitrile. In contrast, a significant fraction of organic constituents in the aged (brown) sample contain one (22%), two (5%), or three (0.5%) three N atoms. The increased population of nitrogen-containing organic compounds is accompanied by a shift in the distribution of O-atom-containing species toward lower numbers, as is shown in Figure 5b. This observation is consistent with reactions r1−r3, which were discussed earlier.

Double-bond-equivalent (DBE) values of neutral molecules were calculated from the experimentally determined elemental formulas using eq 3:

$$\mathrm{DBE} = 1 - \left(\frac{h}{2}\right) + \left(\frac{n}{2}\right) + c \qquad (3)$$

where h, n, and c correspond to the number of H, N, and C atoms in the assigned peaks, respectively. (Note that the ionizing proton

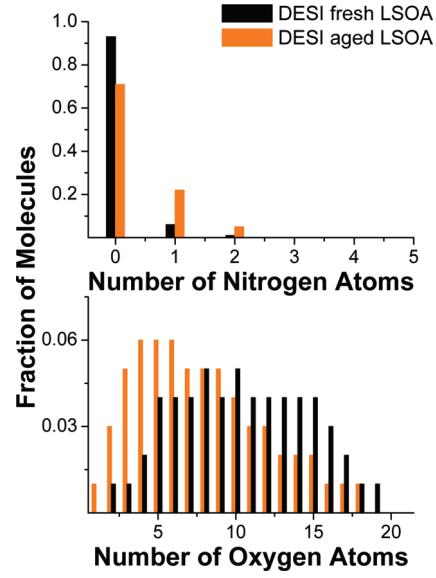

Figure 5. Distribution of the number of N atoms (top) and O atoms (bottom) in identified mass spectral features observed in DESI spectra of fresh (white) and aged (brown) LSOA samples. Black bars correspond to the fresh LSOA sample; orange bars represent the aged LSOA sample.

(80) Varutbangkul, V.; Brechtel, F. J.; Bahreini, R.; Ng, N. L.; Keywood, M. D.; Kroll, J. H.; Flagan, R. C.; Seinfeld, J. H.; Lee, A.; Goldstein, A. H. *Atmos. Chem. Phys.* **2006**, *6*, 2367–2388.
(81) Fenn, M. E. *Environ. Pollut.* **2007**, *146*, 77–91.

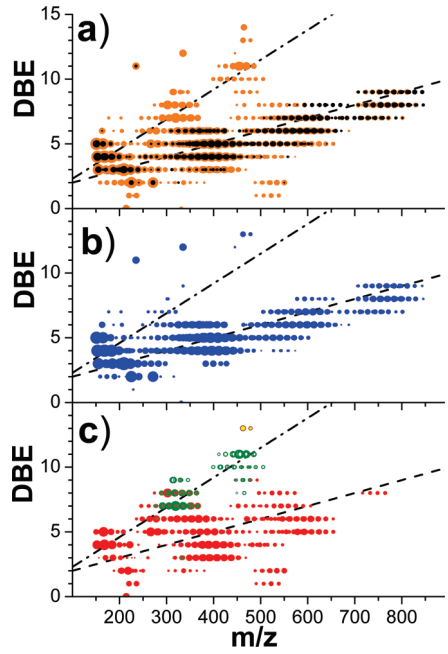

Figure 6. Dependence of the DBE on the *m/z* value for all peaks in DESI spectra. The size of the points is proportional to the logarithm of the peak intensity: (a) comparison of the results obtained for the fresh (white) sample (black dots) and aged (brown) sample (orange dots); (b) data obtained from DESI analysis of the aged sample for species with no N atoms ($n = 0$); (c) data obtained from DESI analysis of the aged sample for species with $n = 1$ (red), $n = 2$ (green), and $n = 3$ (yellow). The dashed line follows the increase in DBE with *m/z* observed for the fresh LSOA sample. The dash-dotted line shows the increase in DBE with *m/z* expected for condensation reactions (see text for detailed discussion).

was subtracted from the number of H atoms). Equation 3 assumes that nitrogen retains its valence of 3 in reactions between NH_3 and SOA constituents; reactions r1−r3 are consistent with this assumption. Figure 6a compares the dependence of DBE values on m/z for all species identified in DESI spectra of the fresh (white) and aged (brown) samples. A major difference between the two samples is observed in the m/z range of 200−500. Specifically, species are observed in the aged (brown) sample with large DBE values that are absent in the spectrum of the fresh (white) sample. These highly conjugated species are of particular interest, because they could be responsible for the observed brown color of the aged sample.

Figure 6b plots DBE as a function of m/z of the identified peaks in the DESI spectrum of aged (brown) sample that do not contain N atoms ($n = 0$), while Figure 6c plots the respective values for nitrogen-containing compounds ($n = 1$−3). Two families of compounds can be clearly distinguished in these plots, which are represented by dashed and dash-dotted lines. The first group of compounds shows a relatively slow increase in DBE, as a function of m/z, and is represented by a dashed line. The increase in DBE shown by the dashed line is consistent with the oligomerization mechanism of LSOA components discussed in the literature.[42] Specifically, Bateman et al. showed that oligomerization of the ozonolysis products of limonene results in the corresponding increase of DBE by approximately two units per addition of a single monomer.[42] The average DBE values for components of the fresh LSOA sample examined in this study (3 for monomers, 5 for dimers, 7 for trimers, and 8 for tetramers) are consistent with the previous work. A similar trend is observed for $n = 0$ molecules in the aged (brown) sample (see Figure 6b). The relatively slow increase in DBE with m/z is rationalized using the oligomerization mechanism that involves reactions between the Criegee intermediate formed in the initial ozone attack on limonene and stable ozonolysis products.[42]

Figure 6c shows that a significant number of aging products containing one N atom follow the same trend in DBE as $n = 0$ molecules. The slow increase in DBE of $n = 1$ molecules with m/z is readily rationalized using reaction r1. Replacement of O with NH has no net effect on the value of DBE but results in a shift in m/z from even to odd values (see Table 2). Remarkably similar DBE values observed for $n = 0$ and the majority of $n = 1$ molecules indicate that a significant number of LSOA constituents undergo the carbonyl-to-imine transformation. Both monomeric and oligomeric species present in the fresh (white) LSOA undergo this transformation, which has only a minor effect on the observed DBE trend.

However, chemical aging also results in the formation of a number of nitrogen-containing dimers and trimers with fairly high DBE values. Condensation reactions between monomers result in the formation of dimers with characteristic DBE values given by the sum of DBE values of the monomeric constituents.[42] The dash-dotted lines in Figure 6 show the estimated trend in DBE values typical for condensation reactions. For example, imine compounds produced via reaction r1 can undergo reactions with carbonyl groups of other molecules present in the LSOA mixture as illustrated by reactions r4:

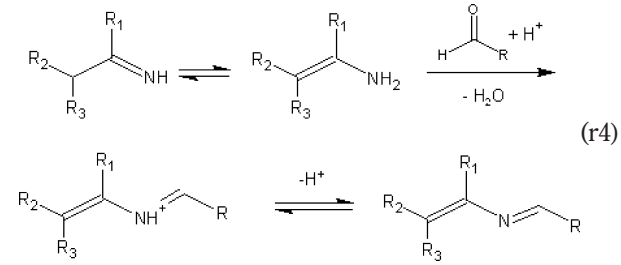

(r4)

These reactions generate higher-molecular-weight oligomeric products through the formation of new C−N bonds linking together the primary ozonolysis products of limonene. Figure 6c shows the presence of several $n = 1$ dimers with large DBE values that are most likely formed through reactions r4. In addition, all $n = 2$ and $n = 3$ species in the aged LSOA sample have large DBE values. Compounds with two N atoms are characterized by average DBE values of 8 for dimers and 11 for trimers. High DBE values observed for $n = 2$ and $n = 3$ compounds indicate that they are formed through condensation reactions similar to reactions r4.

Comparison of DBE values obtained for fresh (white) and aged (brown) samples suggests that two major pathways are responsible for chemical aging of LSOA through reactions with ammonia: (1) transformation of carbonyls to imines via reaction r1, and (2) oligomerization of imines via reaction r4. We propose that condensation reactions associated with substantial increase in DBE are most likely responsible for the formation of products that absorb visible light, whereas the first pathway has a minor effect on the optical properties of LSOA.

Table 3. Intensity of MS/MS Products of Nitrogen-Containing Species in the Aged (Brown) LSOA Sample Normalized to the Most-Abundant Peak

m/z	elemental formula of the ion	DBE	loss of NH_3	loss of H_2O	loss of $H_2O + CO$	loss of C_2H_4O	loss of C_3H_6O	other neutral losses[a]	monomeric fragments[a,b]
152.1067	$C_9H_{14}NO$	4	18	100		60	5		
166.0860	$C_9H_{12}NO_2$	5	2	15	100				
168.1017	$C_9H_{14}NO_2$	4	7	100	21	27	36		
184.0968	$C_9H_{14}NO_3$	4	16	100	22			*−CO (33), −CH₃O (49), −C₂H₄O₂(13)*	
186.1124	$C_9H_{16}NO_3$	3	32	100				*−2H₂O (14), −NH₃−H₂O (11)*	
218.1384	$C_{10}H_{20}NO_4$	2	100					*−NH₃−H₂O (86), −NH₃−2H₂O (43), −NH₃−H₂O−CO (23), −NH₃−C₃H₆O₄ (16)*	
266.1752	$C_{15}H_{24}NO_3$	5		100			32		$C_9H_{14}NO$ (20)
302.1751	$C_{18}H_{24}NO_3$	8		100	10		12	*−CO (11), −C₂H₂O(9), −C₄H₆O(19)*	
304.1545	$C_{17}H_{22}NO_4$	8		100	25		13		$C_9H_{14}NO$ (12)
352.1755	$C_{18}H_{26}NO_6$	7		100				*−2H₂O (14)*	$C_9H_{12}NO$ (27) $C_9H_{12}NO_2$ (41) $C_9H_{14}NO_2$ (20) $C_9H_{14}NO_3$ (7) $C_{13}H_{20}NO_3$ (12)
354.1910	$C_{18}H_{28}NO_6$	6		100				*−2H₂O (15)*	$C_9H_{12}NO$ (24) $C_9H_{12}NO_2$ (34) $C_9H_{14}NO_2$ (14) $C_9H_{14}NO_3$ (20) $C_{13}H_{20}NO_3$ (11)
368.2066	$C_{19}H_{30}NO_6$	6		100				*−2H₂O (10)*	$C_9H_{12}NO$ (11) $C_9H_{12}NO_2$ (23) $C_9H_{14}NO_2$ (20) $C_9H_{14}NO_3$ (17)
317.1860	$C_{18}H_{25}N_2O_3$	8	15	100				*−C₂H₂O₂(11), −NH₃−CO (10), −C₄H₆O(21), −C₃H₆O₂(15)*	$C_{11}H_{13}N_2O$ (20) $C_{12}H_{18}NO$ (19)
319.2017	$C_{18}H_{27}N_2O_3$	7	40	100			68		

[a] Normalized intensities are shown in parentheses. [b] *m/z* of monomeric products: $C_9H_{14}NO$ (152.1066), $C_{11}H_{13}N_2O$ (189.1019), $C_{12}H_{18}NO$ (192.1379), $C_9H_{12}NO$ (150.091), $C_9H_{12}NO_2$ (166.0859), $C_9H_{14}NO_2$ (168.1016), $C_9H_{14}NO_3$ (184.0966), $C_{13}H_{20}NO_3$ (238.1433).

MS/MS experiments were conducted to gain further insight on the structures of nitrogen-containing organic compounds formed in chemical aging experiments. The results are summarized in Table 3. MS/MS spectra of monomeric (C_9-C_{10}) species are dominated by the losses of H_2O, NH_3, and CO. A loss of water is commonly observed for compounds that contain aldehyde, ketone, hydroxyl, and carboxyl groups.[82] The loss of CO is a nonspecific fragmentation pathway observed for carboxylic acids, aromatic aldehydes, and ketones. In contrast, aliphatic aldehydes and ketones decompose via the loss of alkanes or alkenes.[83,84] The loss of NH_3 is characteristic of aliphatic primary amines.[82] MS/MS data obtained for nitrogen-containing monomers suggest that cyclization of these species is unlikely or that cyclic and open structures of these compounds coexist.

In contrast, no NH_3 loss was observed for dimeric ($C_{15}-C_{18}$) compounds that contain one N atom. These species show an abundant loss of water and a number of oxygen-containing organic molecules. The observed fragmentation behavior is consistent with the presence of the heterocyclic N atom or a secondary amine/imine linking two monomeric units. In addition, dissociation of dimeric species results in the formation of several nitrogen-containing monomers, suggesting that the dimerization most likely occurs through reaction r4 and involves nitrogen-containing monomers and oxygenated organic molecules as building blocks. Higher signal intensities in the dimer region observed for the aged sample are consistent with dimerization via reaction r4.

The addition of the second N atom has a significant effect on the structure of nitrogen-containing molecules. The loss of ammonia observed in MS/MS spectra of dimers with two N atoms indicates the presence of one heterocyclic nitrogen (or N atom) linking two monomers, as shown in reaction r4, and one N atom placed by reaction r1 at the periphery of the molecular skeleton.

CONCLUSIONS

In this study, we present the first application of high-resolution DESI-MS for chemical characterization of OA collected on substrates and for studying the effect of chemical aging on the composition of OA. Our results demonstrate several advantages of DESI for high-resolution mass spectrometry analysis of aerosol samples. First, no sample extraction is required for DESI analysis of SOA material deposited on substrates. The Teflon substrates used in this study are large enough to enable multiple analyses of the same sample that are necessary for detailed studies of the kinetics of aerosol aging. Second, DESI enables gentle analysis of chemically unstable aerosol constituents and is much more tolerant to the solvent composition than the more traditional ESI approach. Specifically, chemically labile species present in the aged LSOA sample are readily detected using DESI when a strong acid is added to the solvent. In contrast, most of these labile

(82) Levsel, K.; Schiebel, H. M.; Terlouw, J. K.; Jobst, K. J.; Elend, M.; Preib, A.; Thiele, H.; Ingendoh, A. *J. Mass Spectrom.* **2007**, *42*, 1024–1044.
(83) Sigsby, M. L.; Day, R. J.; Cooks, R. G. *Org. Mass Spectrom.* **1979**, *14*, 273–280.
(84) Wagner, W.; Heimbach, H.; Levsen, K. *Int. J. Mass Spectrom. Ion Processes* **1980**, *36*, 125–142.

species cannot be detected in the ESI analysis that utilizes AcN/TFA as a solvent. The difference between DESI and ESI analysis can be attributed to the short interaction time (of the order of milliseconds) between the analyte and the solvent in DESI that is limited to the residence time in the droplets, compared to the fairly long time (minutes and hours) that the analyte resides in the solvent during ESI analysis. While extraction of the analyte into the pure acetonitrile followed by ESI analysis could help to alleviate some of the problems associated with chemical instability of the organic aerosol constituents, this approach still resulted in measurable decomposition of the labile molecules. DESI-MS analysis of aerosol particles collected on substrates enables detailed studies of the gas-to-particle chemistry relevant to atmospheric aging of aerosols over considerably long periods of time, which cannot be achieved in traditional studies through the use of flow reactors and cloud chambers. Finally, we note that DESI-MS is a promising technique for laboratory studies of atmospherically relevant aging of field-collected aerosols.

We demonstrate that conjugated nitrogen-containing compounds produced through condensation reactions in the aging process are responsible for the absorption of the visible light by the aged LSOA. The formation of the light-absorbing compounds has been attributed to the chemical transformation of carbonyl groups of OA constituents by reactions with ammonia and subsequent oligomerization processes. Because organic molecules containing carbonyl groups are abundant in OA from both biogenic and anthropogenic origin, similar chemical aging processes may be responsible for the atmospheric aging of organic compounds in particulate matter. This study presents an important step toward chemical characterization of the "brown carbon", which is the important and poorly characterized light-absorbing aerosol in the atmosphere. The combination of novel atmospheric-pressure surface-ionization techniques for in situ chemical analysis of surfaces with high-resolution mass spectrometry (HR-MS), as presented in this study, enables detailed characterization of the chemical composition and transformation of particulate matter collected on substrates that is not possible using other techniques.

ACKNOWLEDGMENT

The research described in this manuscript was supported by the intramural research and development program of the W. R. Wiley Environmental Molecular Sciences Laboratory (EMSL), a national scientific user facility sponsored by the U.S. Department of Energy's Office of Biological and Environmental Research. All experiments were performed at EMSL, which is located at Pacific Northwest National Laboratory (PNNL). PNNL is operated by Battelle for the U.S. Department of Energy. P.J.R. acknowledges the support from the Chemical Sciences Division, Office of Basic Energy Sciences of the US DOE. S.A.N. acknowledges support by NSF Grant No. ATM-0831518. D.B. was supported by NSF Grant No. CHE-0909227.

Received for review December 9, 2009. Accepted January 25, 2010.

AC902801F